Journal of Biomolecular NMR, **13:** 375–380, 1999.
KLUWER/ESCOM

Efficient determination of angles subtended by C^{α}-H^{α} and N-H^{N} vectors in proteins via dipole-dipole cross-correlation§

Philippe Pelupessy[a], Elisabetta Chiarparin[a], Ranajeet Ghose[a] & Geoffrey Bodenhausen[a,b,*]
[a]*Section de Chimie, Université de Lausanne, BCH, CH-1015 Lausanne, Switzerland;* [b]*Département de Chimie, Associé au CNRS, Ecole Normale Supérieure, 24 rue Lhomond, F-75231 Paris cedex 05, France*

Received 6 October 1998; Accepted 6 January 1999

Key words: cross-correlation, dihedral angles, dipolar interactions

Abstract

The angle $\Theta_{C^{\alpha}H^{\alpha},NH^{N}}$ subtended by the internuclear vectors $^{13}C^{\alpha}$-H^{α} and ^{15}N-H^{N} in doubly-labeled proteins can be determined by observing the effect of cross-correlation between the dipolar interactions on zero- and double-quantum coherences involving $^{13}C^{\alpha}$ and ^{15}N. Two complementary 2D experiments with the appearance of ^{15}N-H^{N} correlation spectra yield signal intensities that depend on the rate of interconversion through cross-correlated relaxation of in-phase and doubly antiphase zero- and double-quantum coherences. The ratio of the signal intensities in the two experiments bears a simple relationship to the cross-correlation rate, and hence to the angle $\Theta_{C^{\alpha}H^{\alpha},NH^{N}}$. Assuming planarity of the peptide bond, the dihedral angle Ψ (between C^{α} and C') can be determined from the knowledge of $\Theta_{C^{\alpha}H^{\alpha},NH^{N}}$. The experiments are very time-effective and provide good sensitivity and excellent spectral resolution.

Cross-correlation involving interference between two different relaxation mechanisms can provide a great deal of insight into the structure and dynamics of biomolecules. Various experiments (Dalvit et al., 1989; Bull, 1991; Burghardt et al., 1992) have been designed to measure the effects of cross-correlation between two dipolar interactions. Cross-correlation between the fluctuations of chemical shift anisotropy (CSA) and dipolar couplings can also yield information about structure (Tjandra et al., 1997) and local motion (Fischer et al., 1997; Brutscher et al., 1998). Recently, Griesinger and co-workers (Reif et al., 1997) have shown how the relaxation of suitably excited multiple quantum coherences is affected by dipole-dipole cross-correlation, and how this allows one to determine angles subtended between two internuclear vectors that do not share any common nuclei. These experiments bear analogies to recent solid-state methods (Feng et al., 1996; Schmidt-Rohr, 1996). In particular, the relaxation of multiple quantum coherences involving $^{13}C^{\alpha}$(i) and ^{15}N(i+1) of two neighboring amino acids in proteins is affected by cross-correlation between the $^{13}C^{\alpha}$-H^{α} and ^{15}N-H^{N} dipolar interactions. This allows one to determine the dihedral Ψ angle (see Figure 1) that has been inaccessible until recently. In a similar fashion, Kay and co-workers (Yang et al., 1997; Yang and Kay, 1998) determined Ψ angles directly by monitoring the relaxation of multiple quantum coherences involving $^{13}C^{\alpha}$(i) and carbonyl $^{13}C'$(i) of the same amino acid, which is affected by cross-correlation between the $^{13}C^{\alpha}$-$^{1}H^{\alpha}$ dipolar coupling and the carbonyl CSA.

In this communication, we describe how the three-dimensional method of Reif et al. can be replaced by two complementary two-dimensional experiments. Both experiments of Figure 2 begin with a sequence designed to excite multiple quantum coherence (MQC) $4N_xC_x^{\alpha}C_z'$ involving $^{13}C^{\alpha}$(i) and ^{15}N(i+1), which is antiphase with respect to the carbonyl $^{13}C'$(i) (Bax and Ikura, 1991). Instead of letting the multiple quantum coherence evolve in a 3D experiment as described by Reif et al. (1997), a fixed delay T = 25 ms

§Dedicated to Professor Ray Freeman.
*To whom correspondence should be addressed. E-mail: Geoffrey.Bodenhausen@ens.fr

is used to allow relaxation to occur. During this delay, the antiphase term $4N_xC_x^\alpha C_z'$ is partly transformed into a triply antiphase term $16N_yC_y^\alpha C_z'H_z^NH_z^\alpha$ due to cross-correlation between the fluctuations of the $^{13}C^\alpha$-H^α and ^{15}N-H^N dipolar couplings. The rate of this transformation is determined by $R_{C^\alpha H^\alpha,NH^N}$ (Table 1). Experiment A is designed to detect the remaining $4N_xC_x^\alpha C_z'$ term (which plays a role similar to that of the 'source' magnetization in NOESY-like experiments, the amplitude of which is reflected in the intensity of a diagonal peak), while experiment B allows one to measure the amplitude of the $16N_yC_y^\alpha C_z'H_z^NH_z^\alpha$ term at the end of the T interval (this term corresponds to the 'target' magnetization, with an amplitude that is usually measured from a cross peak in NOESY). In both experiments, evolution during T under the chemical shifts of $^{13}C^\alpha$ and ^{15}N is refocused by applying two π pulses in each channel. In experiment A, the first two π pulses are applied to ^{15}N and $^{13}C^\alpha$ after T/4, and two more π pulses at 3T/4, so that the evolution under the $^{13}C^\alpha$-H^α and ^{15}N-H^N scalar couplings is refocused at the end of T. In experiment B, on the other hand, the first two π pulses applied to ^{15}N and $^{13}C^\alpha$ are delayed until $T/4+(8J_{NH^N})^{-1}$ and $T/4+(8J_{C^\alpha H^\alpha})^{-1}$, respectively, in order to convert the term $16N_yC_y^\alpha C_z'H_z^NH_z^\alpha$ into $4N_xC_x^\alpha C_z'$. A second pair of π pulses is applied to $^{13}C^\alpha$ and ^{15}N at T/2 after the first π pulses, so that the chemical shifts of $^{13}C^\alpha$ and ^{15}N are again refocused at the end of T. In addition, a π pulse is applied to ^1H at T/2. In both experiments, the $4N_xC_x^\alpha C_z'$ coherence is transferred back to the amide proton after the T interval. The two complementary 2D experiments A and B yield heteronuclear correlation spectra where the dispersion is determined by the shifts of the amide ^{15}N and H^N in the ω_1 and ω_2 dimensions.

Various cross-correlation pathways (15 in number, Yang and Kay, 1998) are active during T and lead to a conversion of $4N_xC_x^\alpha C_z'$ into a manifold of other terms that are listed in Table 1. These terms can be derived from Redfield theory formulated in the product operator basis. The pathways due to cross-correlation between the $^{13}C^\alpha$ or the ^{15}N CSAs and dipolar couplings involving the $^{13}C^\alpha$, H^α, ^{15}N and H^N nuclei (the last eight terms of Table 1) are cancelled in both experiments by the π pulse applied to ^1H in the middle of T. Thus, these terms need not be considered in the analysis. The remaining terms in Table 1 include six due to dipole–dipole cross-correlation and one due to CSA-CSA cross-correlation. These terms are not averaged out in the experiments. The terms 3–7 in Table 1 are much smaller in magnitude than $R_{C^\alpha H^\alpha,NH^N}$ and do not yield the coherence we choose to detect, namely, $16N_yC_y^\alpha C_z'H_z^NH_z^\alpha$. These rates do not affect our results as long as we are in the linear regime, i.e $R_{ij,kl}T \ll 1$, where $R_{ij,kl}$ is the cross-correlation rate involving the ij and kl dipolar interactions (the term due to CSA-CSA cross-correlation is also in this regime). This leaves us with the first two terms of Table 1. The first term, namely $R_{C^\alpha H^\alpha,NH^N}$ is much larger than the second term, $R_{C^\alpha H^N,NH^\alpha}$ and thus the latter term can be neglected. Note that the other rates could be measured by slightly modifying the proposed pulse sequences.

For a given amino acid, the signals of experiments A and B (which are proportional to the ex-

Table 1. Terms generated from antiphase multiple-quantum (zero- and double-) coherence $4N_xC_x^\alpha C_z'$ due to interference effects between two different relaxation mechanisms[a]

Interaction	Term generated	Rate
$C^\alpha H^\alpha$,NH^N	$-16N_yC_y^\alpha C_z'H_z^N H_z^\alpha$	$R_{C^\alpha H^\alpha,NH^N}$
$C^\alpha H^N$,NH^α	$-16N_yC_y^\alpha C_z'H_z^N H_z^\alpha$	$R_{C^\alpha H^N,NH^\alpha}$
$C^\alpha H^\alpha$,$C^\alpha H^N$	$16N_xC_x^\alpha C_z'H_z^NH_z^\alpha$	$R_{C^\alpha H^\alpha,C^\alpha H^N}$
NH^α,NH^N	$16N_xC_x^\alpha C_z'H_z^NH_z^\alpha$	R_{NH^α,NH^N}
$C^\alpha H^\alpha$,NH^α	$-4N_yC_y^\alpha C_z'$	$R_{C^\alpha H^\alpha,NH^\alpha}$
C^α,N	$-4N_yC_y^\alpha C_z'$	$R_{C^\alpha,N}$
$C^\alpha H^N$,NH^N	$-4N_yC_y^\alpha C_z'$	$R_{C^\alpha H^N,NH^N}$
C^α,$C^\alpha H^\alpha$	$8N_xC_x^\alpha C_z'H_z^\alpha$	$R_{C^\alpha,C^\alpha H^\alpha}$
N,NH^α	$8N_xC_x^\alpha C_z'H_z^\alpha$	R_{N,NH^α}
N,$C^\alpha H^\alpha$	$-8N_yC_y^\alpha C_z'H_z^\alpha$	$R_{N,C^\alpha H^\alpha}$
C^α,NH^α	$-8N_yC_y^\alpha C_z'H_z^\alpha$	R_{C^α,NH^α}
C^α,NH^N	$-8N_yC_y^\alpha C_z'H_z^N$	R_{C^α,NH^N}
N,$C^\alpha H^N$	$-8N_yC_y^\alpha C_z'H_z^N$	$R_{N,C^\alpha H^N}$
C^α,$C^\alpha H^N$	$8N_xC_x^\alpha C_z'H_z^N$	$R_{C^\alpha,C^\alpha H^N}$
N,NH^N	$8N_xC_x^\alpha C_z'H_z^N$	R_{N,NH^N}

[a] Assuming the slow motion limit, only those interactions which have a contribution to the spectral density function at zero frequency, $J_a(0)$, have been considered. The rates $R_{ij,kl}$, $R_{i,jk}$ and $R_{i,j}$ denote dipole-dipole, CSA-dipole and CSA-CSA cross-correlation rates, respectively. These are given by: $R_{ij,kl} = (\mu_0\hbar/2\pi)^2(\gamma_i\gamma_j\gamma_k\gamma_l/r_{ij}^3r_{kl}^3)Y_{20}(\Theta_{ij,kl})J_a(0)$; $R_{i,jk} = (\mu_0\hbar/2\pi)(\gamma_i\gamma_j\gamma_k\Delta\sigma_iB_0/r_{jk}^3)Y_{20}(\Theta_{i,jk})[2J_a(0)/3]$; $R_{i,j} = (\gamma_i\gamma_j\Delta\sigma_i\Delta\sigma_jB_0^2)Y_{20}(\Theta_{i,j})[2J_a(0)/9]$, where $Y_{20}(\Theta) = (3\cos^2\Theta - 1)/2$ and $J_a(0) = 2S^2\tau_c/5$, S^2 is the generalized order parameter (Lipari and Szabo, 1982) and τ_c is the global correlation time (assuming isotropic overall tumbling). The chemical shift tensors have been assumed to be axially symmetric and the Θ's denote the angles between pairs of interactions. The other symbols have their usual meaning.

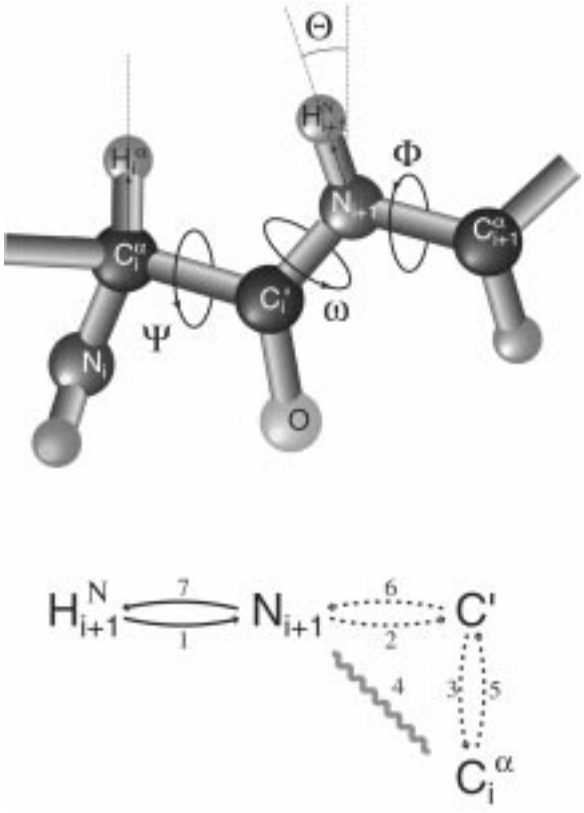

Figure 1. (top) Schematic representation of the backbone of a protein with various dihedral angles. The angle $\Theta_{C^{\alpha}H^{\alpha},NH^{N}}$ subtended between the vectors $^{13}C^{\alpha}$-H^{α} and ^{15}N-H^{N} can be determined with the experiments of Figure 2. (bottom) Antiphase double-quantum coherence $4N_xC^{\alpha}_xC'_z$ is excited starting from H^N_z via several INEPT (dashed arrows) and refocused INEPT (bold arrows) steps. The term $16N_yC^{\alpha}_yC'_zH^N_zH^{\alpha}_z$ is created due to cross-correlation.

pectation values of $4N_xC^{\alpha}_xC'_z$ and $16N_yC^{\alpha}_yC'_zH^N_zH^{\alpha}_z$, respectively) have the following intensities:

$$S_A = K\left[\exp(-R_AT - R_{C^{\alpha}H^{\alpha},NH^{N}}T) + \exp(-R_AT + R_{C^{\alpha}H^{\alpha},NH^{N}}T)\right] \quad (1a)$$

$$S_B = K\left[\exp(-R_AT - R_{C^{\alpha}H^{\alpha},NH^{N}}T') - \exp(-R_AT + R_{C^{\alpha}H^{\alpha},NH^{N}}T')\right] \quad (1b)$$

where R_A is the auto-relaxation rate which need not be determined and K is a common amplitude factor. The period $T' = T - (2J_{NH^N})^{-1} + (2J_{C^{\alpha}H^{\alpha}})^{-1}$ has been defined to account for the fact that the effective $R_{C^{\alpha}H^{\alpha},NH^{N}}$ rate changes sign because of the π pulses applied to the $^{13}C^{\alpha}$ and ^{15}N channels (see Figure 2). The ratio of the signals in Equation 1 has a simple dependence on $R_{C^{\alpha}H^{\alpha},NH^{N}}$:

$$S_A/S_B = \left[\exp(-R_{C^{\alpha}H^{\alpha},NH^{N}}T) + \exp(R_{C^{\alpha}H^{\alpha},NH^{N}}T)\right] / \left[\exp(-R_{C^{\alpha}H^{\alpha},NH^{N}}T') - \exp(R_{C^{\alpha}H^{\alpha},NH^{N}}T')\right] \quad (2a)$$

Since $(T - T') = (2J_{NH^N})^{-1} - (2J_{C^{\alpha}H^{\alpha}})^{-1}$, i.e. typically 2 ms, we have $(T - T')R_{C^{\alpha}H^{\alpha},NH^{N}} \ll 1$, hence

$$S_A/S_B \approx -\coth(R_{C^{\alpha}H^{\alpha},NH^{N}}T') + (T - T')R_{C^{\alpha}H^{\alpha},NH^{N}} \quad (2b)$$

The second term on the right-hand side of Equation 2b is less than 1% of the first, and thus can be neglected. Equation 2b transforms to:

$$S_B/S_A \approx -\tanh(R_{C^{\alpha}H^{\alpha},NH^{N}}T') \quad (2c)$$

This expression is analogous to the one obtained by Tjandra and Bax (1997) in their experiments designed to measure the interference between ^{15}N CSA and ^{15}N-H^N dipolar couplings in proteins.

Assuming planarity of the peptide bond, the backbone dihedral angle Ψ (see Figure 1) is related to the angle $\Theta_{C^{\alpha}H^{\alpha},NH^{N}}$ subtended by the $^{13}C^{\alpha}$-H^{α} and ^{15}N-H^N vectors (Reif et al., 1997):

$$\cos\Theta_{C^{\alpha}H^{\alpha},NH^{N}} = 0.163 + 0.819\cos(\Psi - 119°) \quad (3)$$

The two complementary spectra of doubly labeled human ubiquitin are shown in Figure 3. The relaxation period, T, is set to a multiple of $(J_{C^{\alpha}C^{\beta}})^{-1}$ in order to minimize losses due to this scalar coupling. This causes the residues on the C-terminal side of glycines (which lack C^{β} atoms) to lead to negative signals (filled in black) in experiment A. In addition to this effect, the sign of a cross peak in experiment B depends on the sign of $R_{C^{\alpha}H^{\alpha},NH^{N}}$. In Figure 4, the rates $R_{C^{\alpha}H^{\alpha},NH^{N}}$ calculated with Equation 2c from the intensities in Figure 3 have been plotted against Ψ angles obtained from the X-ray structure of ubiquitin (Vijay-Kumar et al., 1987) using the program Molmol (Konradi et al., 1996). Theoretical curves derived from the expression for $R_{C^{\alpha}H^{\alpha},NH^{N}}$ in Table 1 and

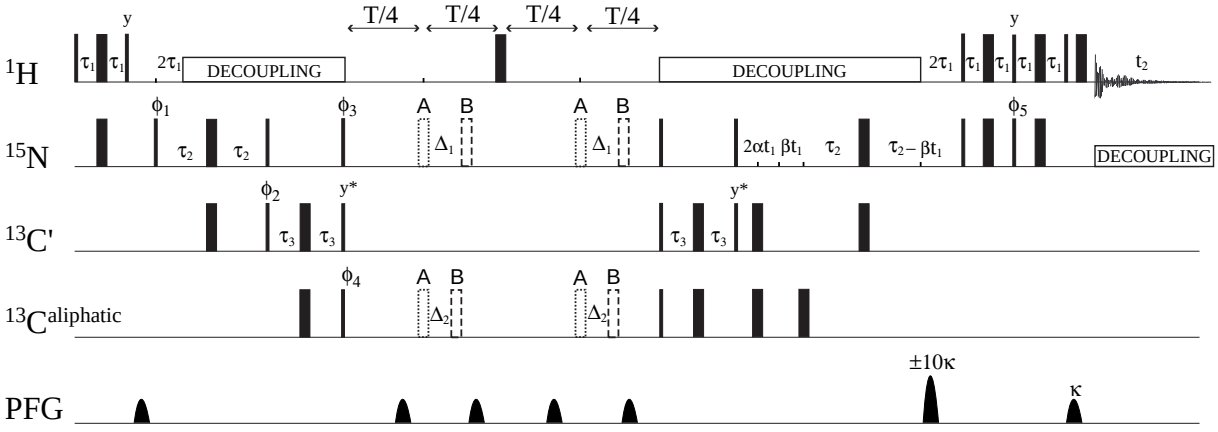

Figure 2. Pulse sequences employed to excite $4N_xC_x^{\alpha}C_z'$ for the measurement of cross-correlation rates due to $^{13}C^{\alpha}$-H^{α} and ^{15}N-H^N dipolar interactions. Narrow and wide bars indicate $\pi/2$ (or $3\pi/2$) and π pulses. The ^{13}C pulses with $3\pi/2$ flip angles have Gaussian shapes (Emsley and Bodenhausen, 1989) of 300 μs duration and the ^{13}C π pulses have shapes of G^3 Gaussian cascades (Emsley and Bodenhausen, 1990a) of 400 μs duration. The delays are $\tau_1 = (4J_{NH^N})^{-1}$, $\tau_2 = (4J_{NC'})^{-1}$ and $\tau_3 = (4J_{C'C^{\alpha}})^{-1}$. The relaxation period T is 25 ms, Δ_1 is set to $(8J_{NH^N})^{-1}$ and Δ_2 to $(8J_{C^{\alpha}H^{\alpha}})^{-1}$. In experiment A the π pulses on the ^{13}C and ^{15}N channels are inserted before these delays (dotted rectangles), while in experiment B they are inserted after these delays (dashed rectangles). The magnetization first evolves during $2\alpha t_1$ in real time, then continues to evolve in the manner of a constant-time experiment to refocus the scalar coupling $J_{NC'}$. The constant β, which must fulfill the condition $2\alpha + 2\beta = 1$, can be chosen to achieve the desired resolution, given by $\beta/(\tau_2 - 2\tau_1)$. Sensitivity is enhanced by echo-antiecho gradient selection (Palmer III et al., 1991). Unless specified otherwise, all pulses are applied along the x-axis. Corrections for Bloch–Siegert shifts (Emsley and Bodenhausen, 1990b) need to be added to the phases marked with stars. The phase cycling is: $\Phi_1 = (x), (-x)$, $\Phi_2 = 2(x), 2(-x)$, $\Phi_3 = 4(x), 4(-x)$, $\Phi_4 = 8(x), 8(-x)$, $\Phi_5 = 16(y), 16(-y)$. Decoupling of the proton and nitrogen channels can be achieved with WALTZ-16 (Shaka et al., 1983) and GARP (Shaka et al., 1985) sequences, respectively.

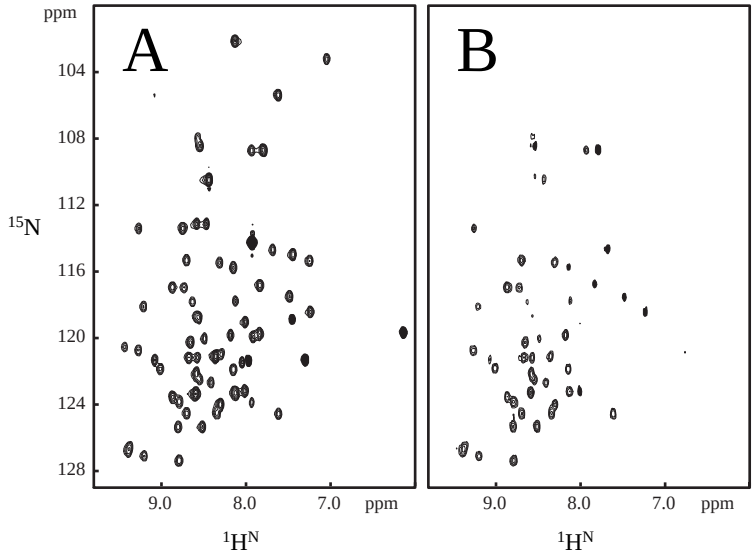

Figure 3. Experimental data for human ubiquitin: (A) ^{15}N-H^N correlation spectrum obtained with experiment A. Negative cross peaks corresponding to amide protons in residues on the C-terminal side of glycines are filled in black. (B) ^{15}N-H^N correlations from experiment B. The ratio of the cross-peak intensities of both experiments gives the dipolar cross-correlation rate $R_{C^{\alpha}H^{\alpha},NH^N}$ between ^{15}N-H^N and $^{13}C^{\alpha}$-H^{α} according to Equation 2c. If peaks are missing in the second experiment, this indicates a vanishing rate. The digital resolution in the ω_1 dimension is 11 Hz, and 128 scans were accumulated for each of the 148 t_1 points, resulting in a total experimental time of 7.5 h per experiment. The experiments have been carried out with a Bruker 400 MHz Avance spectrometer equipped with a triple resonance TBO probe at 303 K with a 1.5 mM sample of ^{15}N- and ^{13}C-labeled human ubiquitin (VLI Research) in H_2O: $D_2O = 9$: 1 buffered at pH = 4.5. All data processing and peak-picking was carried out using the NMRPipe and NMRdraw software (Delaglio et al., 1995).

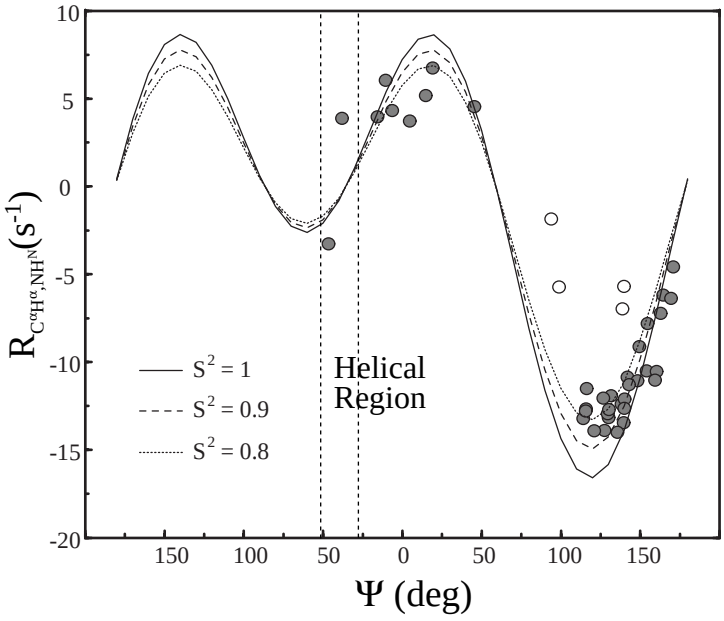

Figure 4. Experimental cross-correlation rates $R_{C^\alpha H^\alpha,NH^N}$ as a function of the backbone angle Ψ, obtained from the X-ray structure of ubiquitin, compared to theoretical curves. The analysis was performed for all non-glycine residues. The correlation time was assumed to be 4 ns. The curves correspond to different order parameters S^2 between 0.8 and 1. The area between vertical dashed lines corresponds to the α-helical region where the corresponding rates are very small because the angle $\Theta_{C^\alpha H^\alpha,NH^N}$ subtended between the vectors $^{13}C^\alpha$-H^α and ^{15}N-H^N is close to 54.7°. The $R_{C^\alpha H^\alpha,NH^N}$ corresponding to the four residues in the C-terminal loop (see text) with small order parameters are indicated by open circles.

Equation 3 are also presented. A global correlation time of 4 ns has been assumed. The experimental points lie mostly between two curves calculated for order parameters $S^2 = 0.8$ and 0.9, most residues in ubiquitin having order parameters in this range (Tjandra and Bax, 1997). In Figure 4, the Ψ areas corresponding to the α-helical regions of ubiquitin indicate $R_{C^\alpha H^\alpha,NH^N}$ values that are close to zero since $\Theta_{C^\alpha H^\alpha,NH^N}$ is close to 54.7°. In general, the absence of a peak in experiment B is a strong indication that the corresponding residue is located in an α-helical region of the protein.The four points indicated by open circles in Figure 4 correspond to rates $R_{C^\alpha H^\alpha,NH^N}$ that are far smaller than those expected from the calculated curves. These points belong to residues 72–75 in the C-terminal loop which have very low order parameters and hence low $R_{C^\alpha H^\alpha,NH^N}$ values. A simple relationship has been assumed to hold between the spectral density functions for cross-correlation $J_{i,j}(0)$ and the auto-correlation spectral density functions $J_a(0)$:

$$J_{i,j}(0) = Y_{20}(\Theta_{i,j})J_a(0) \qquad (4)$$

where $Y_{20}(\Theta_{i,j}) = 1/2(3\cos^2\Theta_{i,j} - 1)$ depends on the angle $\Theta_{i,j}$ between the principal axes of the interactions i and j. This assumption is reasonable for nearly spherical proteins such as ubiquitin (Tjandra et al., 1995).

The two complementary experiments described above provide a very efficient means to measure backbone Ψ-angles. In effect, we propose to drop the third dimension of the experiment described by Reif et al. (1997). It is not necessary to have an evolution period where the zero- and double-quantum coherences are allowed to precess. Our experiments have the same resolution as HSQC spectra and each residue leads to a single peak. The ratio of peak intensities of two experiments that can be recorded in interleaved fashion is fairly reliable. However, the transformation of the term $16N_yC^\alpha_yC'_zH^N_zH^\alpha_z$ into $4N_xC^\alpha_xC'_z$ in experiment B relies on the assumption that all coupling constants $J_{C^\alpha H^\alpha}$ and J_{NH^N} are uniform throughout the protein. Variations of these coupling constants lead to deviations of the signal S_B by a factor $\cos(0.5\pi J_{C^\alpha H^\alpha}/ < J_{C^\alpha H^\alpha} >)\cos(0.5\pi J_{NH^N}/ < J_{NH^N} >)$, which amounts to less than 1% if *both* scalar couplings deviate 5% from the average (indi-

cated by the '<>'). Another source of error could result from the passive $^1J_{C^\alpha N}$ couplings (7–11 Hz) which cause a differential attenuation of the signals in the two experiments. This leads to an overestimation of the signal amplitudes in experiment B. The rates in Figure 4 have been corrected for an average $^1J_{C^\alpha N}$ value of 9 Hz, resulting in a maximum possible error of 2%.

In conclusion, we propose a pair of complementary 2D experiments which enable one to determine the effects of cross-correlation between $^{13}C^\alpha$-H^α and ^{15}N-H^N dipolar interactions on the relaxation of the antiphase multiple quantum coherence $4N_xC_x^\alpha C_z'$. The methodology can be easily extended to measure other cross-correlated relaxation rates. Especially promising are experiments that employ selective pulses on C^α nuclei in order to decouple C^α from C^β (Yang et al., 1998). This allows one to reduce the constant interval T, thus making these schemes applicable to larger biomolecules. In the 3D experiments, however, short constant time evolution periods lead to limited digital resolution in the zero- and double-quantum dimension, thus hampering their actual use (Yang et al., 1998). In our method, the duration of the relaxation interval T is not dictated by the necessity to resolve the lines of the multiplet in the third dimension. Furthermore, if the signals overlap in HSQC spectra, the dispersion of the cross peaks can be improved by inserting an additional evolution period to allow precession of the carbonyl $^{13}C'$ nuclei, which have favorable relaxation properties.

Acknowledgements

This work was supported by the Fonds National de la Recherche Scientifique (FNRS) and the Commission pour la Technologie et l'Innovation (CTI) of Switzerland, and by the Centre National de la Recherche Scientifique (CNRS) of France. We would like to thank Dr. Catherine Zwahlen for stimulating discussions.

References

Bax, A. and Ikura, M. (1991) *J. Biomol. NMR*, **1**, 99–104.
Brutscher, B., Bremi, T., Skrynnikov, N., Brüschweiler, R. and Ernst, R.R. (1998) *J. Magn. Reson.*, **130**, 346–351.
Bull, T.E. (1991) *J. Magn. Reson.*, **93**, 596–602.
Burghardt, I., Konrat, R. and Bodenhausen, G. (1992) *Mol. Phys.*, **75**, 467–486.
Dalvit, C. and Bodenhausen, G. (1989) *Chem. Phys. Lett.*, **161**, 554–560.
Delaglio, F., Grzesiek, S., Vuister, G.W., Zhu, G., Pfeifer, J. and Bax, A. (1995) *J. Biomol. NMR*, **6**, 277–293.
Emsley, L. and Bodenhausen, G. (1989) *J. Magn. Reson.*, **93**, 151–170.
Emsley, L. and Bodenhausen, G. (1990a) *Chem. Phys. Lett.*, **165**, 469–476.
Emsley, L. and Bodenhausen, G. (1990b) *Chem. Phys. Lett.*, **168**, 297–303.
Feng, X., Lee, Y.K., Sandström, D., Edén, M., Maisel, H., Sebald, A. and Levitt, M.H. (1996) *Chem. Phys. Lett.*, **257**, 314–320.
Fischer, M., Zeng, L., Pang, Y., Hu, W., Majumdar, A. and Zuiderweg, E.R.P. (1997) *J. Am. Chem. Soc.*, **119**, 12629–12642.
Konradi, R., Billeter, M. and Wüthrich, K. (1996) *J. Mol. Graphics*, **14**, 51–55.
Lipari, G. and Szabo, A. (1982) *J. Am. Chem. Soc.*, **104**, 4546–4558.
Palmer III, A.G., Cavanagh, J., Wright, P.E. and Rance, M. (1991) *J. Magn. Reson.*, **93**, 151–170.
Reif, B., Hennig, M. and Griesinger, C. (1997) *Science*, **276**, 1230–1233.
Schmidt-Rohr, K. (1996) *J. Am. Chem. Soc.*, **118**, 7601–7603.
Shaka, A.J., Keeler, J., Frenkiel, T. and Freeman, R. (1983) *J. Magn. Reson.*, **52**, 335–338.
Shaka, A.J., Barker, P.B. and Freeman, R. (1985) *J. Magn. Reson.*, **64**, 547–552.
Tjandra, N., Feller, S.E., Pastor, R.W. and Bax, A. (1995) *J. Am. Chem. Soc.*, **117**, 12562–12566.
Tjandra, N., Szabo, A. and Bax, A. (1996) *J. Am. Chem. Soc.*, **118**, 6986–6991.
Tjandra, N. and Bax, A. (1997) *J. Am. Chem. Soc.*, **119**, 8076–8082.
Vijay-Kumar, S., Bugg, C.E. and Cook, C.J. (1987) *J. Mol. Biol.*, **194**, 531–534.
Yang, D., Konrat, R. and Kay, L.E. (1997) *J. Am. Chem. Soc.*, **119**, 11938–11940.
Yang, D., Gardner, K.H. and Kay, L.E. (1998) *J. Biomol. NMR*, **11**, 213–220.
Yang, D. and Kay, L.E. (1998) *J. Am. Chem. Soc.*, **120**, 7905–7915.